Journal of Cerebral Blood Flow & Metabolism (2014) 34, 380–388

www.jcbfm.com

ORIGINAL ARTICLE

Cerebral oxygen metabolism in neonates with congenital heart disease quantified by MRI and optics

Varsha Jain[1,7], Erin M Buckley[2,3,7], Daniel J Licht[2], Jennifer M Lynch[3], Peter J Schwab[2], Maryam Y Naim[4], Natasha A Lavin[5], Susan C Nicolson[6], Lisa M Montenegro[6], Arjun G Yodh[3] and Felix W Wehrli[1]

Neonatal congenital heart disease (CHD) is associated with altered cerebral hemodynamics and increased risk of brain injury. Two novel noninvasive techniques, magnetic resonance imaging (MRI) and diffuse optical and correlation spectroscopies (diffuse optical spectroscopy (DOS), diffuse correlation spectroscopy (DCS)), were employed to quantify cerebral blood flow (*CBF*) and oxygen metabolism ($CMRO_2$) of 32 anesthetized CHD neonates at rest and during hypercapnia. Cerebral venous oxygen saturation (S_vO_2) and *CBF* were measured simultaneously with MRI in the superior sagittal sinus, yielding global oxygen extraction fraction (*OEF*) and global $CMRO_2$ in physiologic units. In addition, microvascular tissue oxygenation (StO_2) and indices of microvascular *CBF* (BFI) and $CMRO_2$ ($CMRO_{2i}$) in the frontal cortex were determined by DOS/DCS. Median resting-state MRI-measured *OEF*, *CBF*, and $CMRO_2$ were 0.38, 9.7 mL/minute per 100 g and 0.52 mL O_2/minute per 100 g, respectively. These *CBF* and $CMRO_2$ values are lower than literature reports for healthy term neonates (which are sparse and quantified using different methods) and resemble values reported for premature infants. Comparison of MRI measurements of global S_vO_2, *CBF*, and $CMRO_2$ with corresponding local DOS/DCS measurements demonstrated strong linear correlations ($R^2 = 0.69$, 0.67, 0.67; $P < 0.001$), permitting calibration of DOS/DCS indices. The results suggest that MRI and optics offer new tools to evaluate cerebral hemodynamics and metabolism in CHD neonates.

Journal of Cerebral Blood Flow & Metabolism (2014) **34,** 380–388; doi:10.1038/jcbfm.2013.214; published online 11 December 2013

Keywords: cerebral blood flow; cerebral hemodynamics; diffuse optics; MRI; near-infrared spectroscopy; neonatal ischemia

INTRODUCTION

Congenital heart disease (CHD) affects ~35,000 neonates each year in the United States. These patients suffer both short- and long-term neurologic sequelae. Periventricular leukomalacia is the most common cerebral injury found in this population. This type of injury is characterized by focal necrosis in the periventricular white matter, and it is associated with pyknotic glial nuclei and reactive gliosis.[1,2] During the early stages of brain development, the oligodendrocyte (brain glial cells) precursors are metabolically very active and highly susceptible to injury from reduced blood flow and oxygen delivery. Hence, hypoxia–ischemia has been implicated as a major cause of this injury in CHD neonates.

Periventricular leukomalacia leads to impaired myelination and has been linked to worse neurodevelopmental outcomes in premature infants and postulated to cause (at least in part) the impaired cognition and cerebral palsy commonly seen in this cohort of infants with CHD.[3,4] Quantification of the hemodynamic and metabolic state of these neonates via measurements of cerebral blood flow (*CBF*) and the cerebral metabolic rate of oxygen consumption ($CMRO_2$) should provide valuable information toward understanding the interaction between cardiac pathophysiology and subsequent cerebral health. Potentially, such new knowledge could help predict and prevent adverse outcomes.

Currently, few noninvasive diagnostic modalities exist for the study of cerebral hemodynamics and metabolism. Commercially available near-infrared spectroscopy devices are being used for assessing microvascular oxygen saturation in some cardiac intensive care units. Their major advantage is the ease of acquisition and capability for continuous bedside monitoring. Nevertheless, although near-infrared spectroscopy measurements of blood oxygen saturation have been used to infer cerebral perfusion and metabolism, the method's utility requires further evaluation. Transcranial Doppler ultrasound has also been used in this clinical population.[5] The method measures blood velocity in feeder arteries, which is difficult because of the small size of the vessels in neonates[6] and because the measurements are highly operator dependent.

Licht *et al*[7] applied arterial spin labeling (ASL) magnetic resonance imaging (MRI) to measure *CBF* in neonates. The method provides perfusion maps of the brain but is hampered by the extremely low *CBF* in this population. Alternatively, phase-contrast (PC) MRI yields velocity measurements in the major feeder or drainage vessels and therefore provides global *CBF* even for low-flow velocities. This method is well validated and has been used to study flow for more than 2 decades.[8] However, while quantification of total brain blood flow is relatively straightforward, measurement of cerebral venous oxygen saturation (S_vO_2), the other key component

[1]Department of Radiology, University of Pennsylvania Medical Center, Philadelphia, Pennsylvania, USA; [2]Division of Neurology, Children's Hospital of Philadelphia, Philadelphia, Pennsylvania, USA; [3]Department of Physics and Astronomy, University of Pennsylvania, Philadelphia, Pennsylvania, USA; [4]Division of Critical Care Medicine, Children's Hospital of Philadelphia, Philadelphia, Pennsylvania, USA; [5]Division of Respiratory Therapy, Children's Hospital of Philadelphia, Philadelphia, Pennsylvania, USA and [6]Division of Cardiothoracic Anesthesia, Children's Hospital of Philadelphia, Philadelphia, Pennsylvania, USA. Correspondence: Dr FW Wehrli, Department of Radiology, University of Pennsylvania Medical Center, 1 Founder, MRI Education Center, 3400 Spruce Street, Philadelphia, PA 19104, USA.
E-mail: wehrli@mail.med.upenn.edu
This work was supported by National Institutes of Health (R21 HL088182: PI, Dr Wehrli; R01 NS072338: PI, Dr Licht; K23 NS052380: PI, Dr Licht; R01 NS060653: PI, Dr Yodh; P41 EB015893: Dr Yodh; T32NS007413: Dr Buckley), by the Dana Foundation (PI, Dr Licht), and by the Steve and Judy Wolfson Family Trust (PI, Dr Licht).
[7]These authors contributed equally to this work.
Received 31 July 2013; revised 30 October 2013; accepted 4 November 2013; published online 11 December 2013

required to quantify $CMRO_2$, is not. Two different approaches have emerged to address the quantification of S_vO_2, both making use of the venous blood's paramagnetism: (1) Transverse relaxation-based methods (for example, T_2 Relaxation Under Spin Tagging TRUST,[9] and Quantitative Imaging of Extraction of Oxygen and Tissue Consumption, QUIXOTIC[10]), and (2) susceptometric techniques that quantify the blood's magnetic susceptibility, which is linearly related to deoxyhemoglobin concentration[11–13] (for example phase-based measurement of regional oxygen concentration, PROM[14]).

In this study, we employed recently developed MRI and optical methods for quantification of *CBF* and oxygen metabolism ($CMRO_2$). The MRI method measures venous blood oxygen saturation in the superior sagittal sinus (SSS) via MRI susceptometry[11–13] and, simultaneously, *CBF* by PC MRI; the combination yields global $CMRO_2$ in absolute physiologic units. The optical method utilizes a portable bedside instrument to probe regional microvascular tissue oxygenation, perfusion, and metabolism in the frontal cortex.[15]

The primary aim was to quantify *CBF*, oxygen extraction fraction (*OEF*), and $CMRO_2$ at rest and in response to hypercapnia in a cohort of CHD neonates at risk for perinatal hypoxic–ischemic injury by means of concurrent measurements, with MRI and optical techniques. Further, we aimed to derive calibration factors to convert optical indices of cerebral hemodynamic variables into absolute units for this population group on the basis of the measures obtained by global MRI quantification of blood flow and $CMRO_2$.

MATERIALS AND METHODS

All full-term newborn infants with complex CHD admitted to The Children's Hospital of Philadelphia were screened for participation in this study (approved by the Institutional Review Board, which adheres to the regulations of the Common Rule and the Food and Drug Administration's Institutional Review Board and human subject regulations). Inclusion criteria included gestational age of 40 ± 4 weeks and an intention to undergo surgery with cardiopulmonary bypass during the first month of life. Exclusion criteria included the following: small for gestational age (<2 kg), a history of neonatal depression (5 minutes Apgar score <5 or umbilical cord pH <7.0), or evidence of other end-organ dysfunction. In addition, subjects who experienced preoperative cardiac arrest requiring chest compressions were excluded from the study.

On the morning of the patient's scheduled cardiac surgery, the patient was anesthetized with 5 to 10 μg/kg of fentanyl, paralyzed with 0.2 mg/kg of pancuronium, and prepared for surgery, including nasotracheal intubation, and arterial line placement. The study protocol has been described previously[15,16] and the timeline is illustrated in Figure 1. Briefly, once the anesthetized and paralyzed patient was stabilized and baseline DOS measurements were made while obtaining vascular access, patients were brought to the MRI scanner where a second MRI-compatible, non-invasive optical probe was placed on the forehead for continuous DOS/DCS monitoring. After a 15-minute baseline stabilization period of room air ventilation and an arterial blood gas documenting a partial pressure of carbon dioxide of 40 ± 4 mm Hg, MRI was performed to yield S_vO_2 and *CBF*, from which $CMRO_2$ could be derived. Carbon dioxide was then added to the room air mixture to achieve a fraction of inspired CO_2 of $\sim$3% for a 30-minute hypercapnic period to permit gas equilibration. Magnetic resonance imaging and DOS/DCS data were acquired simultaneously at the end of this 30-minute hypercapnic period. During the period of equilibration, an anatomic and volumetric brain MRI was obtained.

Heart rate, cuff blood pressure, peripheral oxygen saturation, and fraction of inspired CO_2 were monitored and recorded throughout the duration of the study. Arterial blood samples obtained at the start of the baseline period and at the end of the hypercapnia period were used to document that the desired conditions were achieved and to assess arterial oxygen saturation (SaO_2) and hemoglobin (Hb) concentration. Blood samples were analyzed using an i-STAT handheld blood analyzer for partial pressure of carbon dioxide (Abbott Laboratories, Princeton, NJ, USA) and an AVOXimeter 1000E co-oximeter for SaO_2 and Hb (A-VOX Systems, San Antonio, TX, USA).

Magnetic Resonance Imaging Measurements

Cerebral venous oxygen saturation quantification via MR susceptometry relies on the relative magnetic susceptibility difference, $\Delta\chi$, between intravascular blood in the SSS and surrounding tissue. This susceptibility difference is a function of blood oxygenation level causing a perturbation in the local magnetic field; with intravascular water protons sensing a slightly larger magnetic field than those in the surrounding tissue. These magnetic field shifts, and hence the oxygenation level of blood, can be quantified by measuring the phase (ϕ)of the MRI signal. For quantification of S_vO_2 the vessel of interest, i.e., the sagittal sinus, is modeled as a long paramagnetic cylinder[11,12] and S_vO_2 is determined as

$$S_vO_2 = \left[1 - \frac{2\ \Delta\phi}{\gamma\ \Delta\chi_{do}\ B_0 \cdot (\cos^2\theta - \frac{1}{3}) \cdot Hct\ \Delta TE}\right] 100 \quad (1)$$

where γ is the gyromagnetic ratio of water protons (42.576 MHz/T), $\Delta\phi$ is the average phase difference between intravascular blood and surrounding tissue, *Hct* is the blood hematocrit, and θ is the tilt angle of the vessel with respect to the main field, B_o. $\Delta\phi$ is given as

$$\Delta\phi = \gamma\ \Delta B\ \Delta TE \quad (2)$$

Here, ΔB is the incremental field inside the vessel relative to that of the adjacent tissue, and ΔTE is the inter-echo spacing between two gradient-recalled echoes. $\Delta\chi_{do}$ is the susceptibility difference in p.p.m. (SI units) between fully deoxygenated and oxygenated erythrocytes.[17]

Total *CBF* was quantified by PC MRI,[8] a standard technique for measuring blood flow velocity in the SSS, from which *CBF* was calculated by multiplying average velocity in the vessel by the cross-sectional area. As the SSS is known to drain 45% of the total brain blood volume,[18,19] it is

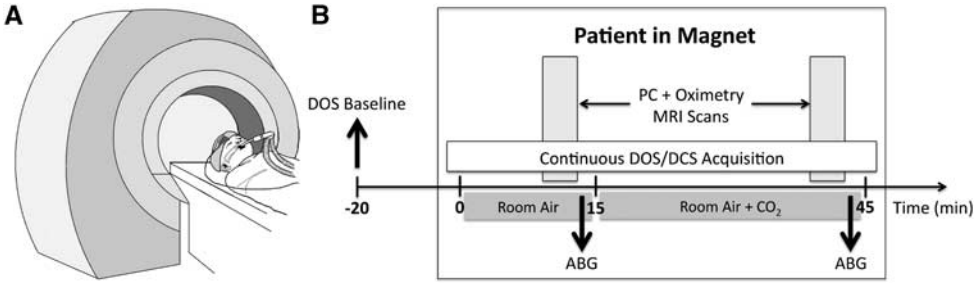

Figure 1. (**A**) Sketch of an anesthetized and intubated patient entering the scanner with magnetic resonance imaging (MRI) compatible optical probe secured to the forehead. (**B**) Timeline of study protocol. Baseline diffuse optical spectroscopy (DOS) measures of deoxy-, oxy-, and total Hb concentrations (HbR, HbO_2, THC, respectively) and tissue oxygen saturation (StO_2) were obtained outside the MRI scanner. Subsequently, the patient was placed in the magnet first inhaling room air for 15 minutes; followed by addition of CO_2 to the gas mixture (fraction of inspired CO_2, 3%). Diffuse optical spectroscopy and diffuse correlation spectroscopy (DCS) data were acquired continuously in-magnet over this entire time period. Oximetry and phase-contrast MRI scans (1 minute in duration) were taken in-magnet at baseline and during hypercapnia. Arterial blood gases (ABG) were also obtained during room air and hypercapnia conditions. PC, phase-contrast.

straightforward to convert *CBF* measurements obtained in SSS to global *CBF* values (in mL/100 g per minute).

Finally, global steady-state cerebral metabolic rate of oxygen consumption ($CMRO_2$, mL O_2/100 g per minute) was calculated via Fick's equation:

$$CMRO_2 = C_a \quad CBF \quad OEF \qquad (3)$$

where C_a is the arterial oxygen concentration in mL O_2/dL blood) and was determined in each subject as $C_a = 1.39 \quad S_aO_2 \quad Hgb$, and *OEF* is the oxygen extraction fraction. S_aO_2 and *Hb* were determined from arterial blood samples. Oxygen extraction fraction was calculated as

$$OEF = \frac{SaO_2 - S_vO_2}{SaO_2} \qquad (4)$$

Magnetic Resonance Imaging Protocol

All images were acquired on a 1.5T Avanto MRI system (Siemens Medical Systems, Malvern, NJ, USA) using a 12-channel head coil. An axial gradient-echo localizer scan was used to choose the straightest section of the vessel of interest (SSS) and to estimate the tilt angle θ of the SSS with respect to B_0 from the coordinates of the centroid of the vessel at two axial locations. A gradient-echo pulse sequence was used for simultaneous measurement of S_vO_2 and *CBF* in the SSS. Specifically, S_vO_2 was quantified using MRI susceptometry-based oximetry and *CBF* via PC MRI. Details on the pulse sequence are in Jain *et al.*[13,20]

The scan parameters were as follows: voxel size = 1 1 5 mm^3, field of view = 112 mm 112 mm, flip angle = 25°, pulse repetition time = 35 milliseconds, echo spacing = 4.16 milliseconds for S_vO_2 quantification, and voxel size = 0.85 0.85 5 mm^3, VENC (parameter determining maximum measurable velocity) = 10 cm/second during normocapnia and 20 cm/second during hypercapnia for *CBF* quantification, number of signal averages = 3, total scan time ~1 minute.

Anatomic T_1- and T_2-weighted high-resolution MRI was performed and neonatal brain volumes were estimated from the resulting images using standard segmentation techniques to obtain *CBF* and $CMRO_2$ in conventional units of mL/minute per 100 g and mL O_2/100 g per minute, respectively.

Relative change in *CBF* (%Δ*CBF*) due to hypercapnia was quantified as a ratio, i.e.,

$$\%\,\Delta CBF = \frac{CBF_{CO_2} - CBF_{\text{room air}}}{CBF_{\text{room air}}} \quad 100\ \% \qquad (5)$$

where the subscript indicates data acquired during the hypercapnic (CO_2) or room air breathing conditions in-magnet. Similar formulas were used to quantify relative changes in *OEF* (i.e., %Δ*OEF*) and $CMRO_2$ (i.e., %Δ$CMRO_2$). Change in S_vO_2 was quantified as the difference between hypercapnic and room air values.

Diffuse Optical and Diffuse Correlation Spectroscopy

DOS and DCS, respectively use near-infrared light to noninvasively probe static and dynamic optical properties of cortical brain tissue microvasculature. These techniques are described in Durduran *et al.*[21] and the specific protocol and measurement details for the present study is detailed in references[15,16] and in Appendix 1. In brief, frequency-domain DOS enables quantification of absolute regional (microvascular) cerebral oxy- and deoxy-hemoglobin concentration (HbO_2 and HbR, respectively, in μmol/L) using photon diffusion theory[21] From this information, total Hb concentration ($THC = HbO_2 + HbR$, in μmol/L), microvascular tissue oxygenation ($StO_2 = HbO_2/THC \quad 100\%$), *OEF*, and cerebral blood volume (*CBV*, in mL/100 g)[22] are readily derived (see Appendix 1).

Diffuse correlation spectroscopy monitors regional microvascular *CBF* noninvasively without the use of exogenous tracers.[21,23] Diffuse correlation spectroscopy quantifies temporal fluctuations in reflected light intensity at points on the tissue surface, which are primarily caused by moving red blood cells.[21] A tissue blood flow index (BFI, cm^2/second) is derived from these temporal fluctuations. Previous studies have shown that changes of BFI relative to a baseline are strongly correlated with changes in *CBF* relative to baseline values measured by other *CBF* techniques.[15,21,24]

Diffuse Optical Spectroscopy and Diffuse Correlation Spectroscopy Instrumentation and Study Protocol

A schematic of the measurement protocol is provided in Figure 1, and further details are given in Appendix 1. First, baseline DOS measurements of absolute tissue physiologic parameters, i.e., HbR, HbO_2, THC, and StO_2 were made on the patient's forehead while the subject was sedated, stabilized, and while vascular access was obtained outside the MRI scanner.[16]

Next, the patient was placed in the MRI scanner; continuous (0.13 Hz) DCS measurements of tissue BFI as well as DOS measurements of changes in HbO_2 and HbR with respect to preMRI values were made by a separate optical probe that employed a single source-detector separation at 2.5 cm as described in Durduran *et al* and Buckley *et al*[15,24] (see Figure 2 for sample time series of DOS data obtained in the MRI scanner). For comparison with the MRI data and to assess the effects of hypercapnia, mean values of all parameters were calculated for each patient by averaging these parameters during the ~1-minute room-air and hypercapnia MRI scans. Absolute hypercapnic *CBV*, *OEF*, and StO_2 were also quantified (see Appendix 1).

Finally, DOS-based measurements of StO_2 and DCS-based measurements of BFI were combined with S_aO_2 and *Hb* obtained from arterial blood samples to yield baseline and hypercapnic $CMRO_{2i}$ using equation (5). Relative changes in *OEF*, BFI, and $CMRO_{2i}$ in response to hypercapnia, i.e. %Δ*OEF*, %ΔBFI, and %Δ$CMRO_{2i}$, were computed using formulas analogous to equation (4). Changes in StO_2 (ΔStO_2) were quantified as a difference between its hypercapnic and room air values.

Statistical Analysis

Paired Wilcoxon signed-rank tests were used to determine whether cerebral hemodynamic parameters during hypercapnia differed from baseline levels. Baseline MRI measurements of S_vO_2, *CBF*, and $CMRO_2$, as well as relative and absolute changes during hypercapnia, were compared with optical measurements (StO_2, BFI, and $CMRO_{2i}$) using linear correlation by computing the Pearson's correlation coefficient. All analyses were performed using the R statistical package (Revolution Analytics), version 2.11; associated *P* values represent the significance of two-sided tests.

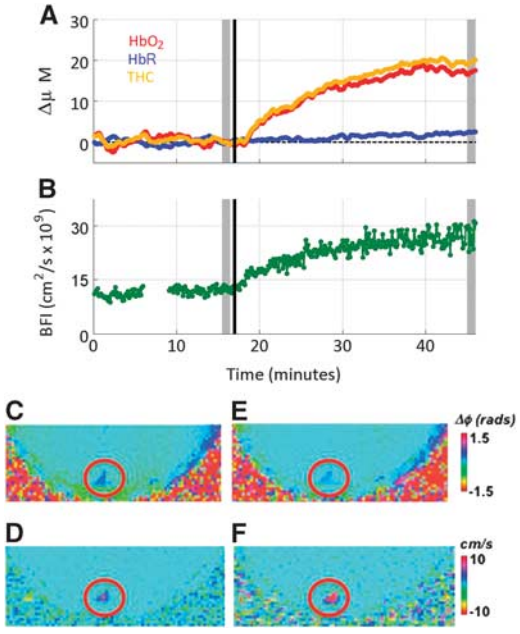

Figure 2. Example time series showing diffuse optical spectroscopy (DOS) data (**A**) and diffuse correlation spectroscopy (DCS) data (**B**) obtained from a typical subject. The patient inhaled room air for approximately 15 minutes, at which time (denoted by black vertical line) CO_2 was added to the room air mixture. Typical parametric magnetic resonance (MR) images obtained at baseline (**C**, **D**) and hypercapnia (**E**, **F**) obtained during the period denoted by shaded gray rectangles. (**C**, **E**) Phase-difference images used for calculating venous oxygen saturation (S_vO_2) and, (**D**, **F**) velocity maps, both acquired in the superior sagittal sinus (SSS, red circle). BFI, blood flow index; THC, total hemoglobin concentration.

RESULTS

Thirty-three patients were consented for this study. One patient was consented but not studied, thus the total cohort consisted of 32 patients; 13 had hypoplastic left heart syndrome, 13 had transposition of the great arteries, 1 had tricuspid atresia with ventricular septal defect and transposition of the great arteries, four had Tetralogy of Fallot, and one had aortic stenosis with arch hypoplasia and a ventricular septal defect. Table 1 lists the median and interquartile range values of the age, weight, gestational age, gender, and head circumference for the entire cohort ($N = 32$). Patients were all full term and measurements were obtained at a median age of 4 days of life (range: 2 to 12 days).

Figure 2 illustrates a sample time series of DOS and DCS data, i.e. ΔHbR, ΔHbO_2, ΔTHC, and BFI as a function of time (Figures 2A and 2B). Figures 2C–2F, depict the phase-difference MR images, obtained during the time period denoted by gray- shaded rectangles in Figures 2A and 2B; these data were used for calculating S_vO_2 and *CBF* at rest and in response to hypercapnia. The decreased contrast in the SSS in the image is used for calculating S_vO_2 (Figures 2C and 2E), and the increased contrast in the velocity maps (Figures 2D and 2F) indicate increased oxygenation level and blood flow velocity in response to hypercapnia.

The median (interquartile range) MRI-measured baseline *OEF*, S_vO_2, *CBF* and $CMRO_2$ as well as DOS/DCS-measured baseline *OEF*, StO_2, BFI, *CBV* and $CMRO_{2i}$ in the cohort are reported in Table 2 (StO_2 values in 14 babies from the present cohort were published previously in conjunction with a study evaluating postoperative changes in near-infrared spectroscopy parameters[16]). Note substantial variation across subjects was observed among all measured resting-state variables. Median baseline $CMRO_2$ was 0.49 mL O_2/minute per 100 g, but it ranged from a minimum of 0.28 to a maximum of 1.17 mL O_2/minute per 100 g across the patient population. Interestingly, baseline $CMRO_2$ was highly linearly correlated with baseline *CBF* as measured by both MRI ($R = 0.70$, $P < 0.001$) and DOS/DCS ($R = 0.78$, $P < 0.001$).

The median increase in partial pressure of carbon dioxide during hypercapnia was 24.9 mm Hg (18.8, 31.2); commensurate with an increase in *CBF* and decrease in *OEF*, as measured by both MRI and optics (all $P < 0.001$, Table 2). Cerebrovascular reactivity, i.e., the fractional change in *CBF* relative to the change in partial pressure of carbon dioxide, was measured by MRI to be 5.02 (3.13, 6.65) %/mm Hg and by DCS to be 3.01 (1.88, 3.94) %/mm Hg. Population-averaged changes in $CMRO_2$ during hypercapnia were not observed by MRI or by DOS/DCS ($P = 0.65$, 0.70, respectively, Table 2). However, individual patients demonstrated a wide range of responses, showing both increases as large as 160% and decreases of as much as 80% in $CMRO_2$.

As seen in Figure 3 and summarized in Table 3, a significant linear correlation was observed between resting-state (baseline) MRI-based absolute measurements of S_vO_2, *CBF*, and $CMRO_2$ and the corresponding DOS/DCS measurements of StO_2, BFI, and $CMRO_{2i}$ ($R^2 = 0.71$, 0.67, 0.60; all $P < 0.001$). Correlation between StO_2 and S_vO_2 was nearly one-to-one with a slope (95% CI) of 0.98 (0.73, 1.24). Using the linear relationship between DCS-measured BFI and MRI-measured *CBF*, we obtained the following calibration coefficients for this cohort, i.e., for conversion of BFI (in units of 10^{-9} cm^2/second) into absolute physiologic units of mL/100 g per minute: $CBF = 1.70 \quad BFI + 2.21$, with 95% confidence intervals of the slope and intercept of (1.20, 2.20) and (-3.68, 8.09), respectively. Similarly, coefficients were obtained to convert $CMRO_{2i}$ (in units of 10^{-7} mL O_2/dL cm^2/second) to physiologic units of mL O_2/100 g per minute: $CMRO_2 = 2.49 \quad CMRO_{2i} - 0.12$, with 95% confidence intervals of the slope and intercept of (1.66, 3.31) and (-0.64, 0.41), respectively.

As depicted in Figure 4, strong correlations were also observed between MRI-measured changes during hypercapnia of S_vO_2, $\%\Delta CBF$ and $\%\Delta CMRO_2$ compared with DOS/DCS measurements of changes in StO_2, $\%\Delta$BFI, and $\%\Delta CMRO_{2i}$ ($R^2 = 0.82$, 0.65, 0.30; all $P < 0.01$); and slopes (95% CI) of 0.88 (0.71, 1.05), 1.03 (0.72, 1.34), and 0.57 (0.01, 1.13), respectively were noted. Bland–Altman plots revealed all data points to lie within two s.d. values of the mean

Table 1. Patient demographics

Parameter	*Median (IQR)*
Age (days)	4 (3, 5)
Weight (kg)	3.4 (3.1, 3.8)
Gestational age (weeks)	38.9 (38.1, 39.3)
Gender (male:female)	17:15
Head circumference (cm)	34.2 (33.5, 35.0)

IQR, interquartile range.

Table 2. Physiologic parameters during baseline and hypercapnia

Parameter	*Baseline*	*Hypercapnia*	*Change from baseline (%)*	P-*value*
*S_aO_2 (%)	89.3 (84.5, 92.3)	84.2 (79.1, 88.7)	-3.3 (-8.4, -0.5)	<0.001
**Hb* (g/dL)	13.5 (12.4, 14.2)	13.7 (12.8, 15.2)	0.6 (-3.5, 5.4)	0.28
C_a (mL/dL)	16.4 (15.1, 17.8)	15.9 (13.6, 17.6)	-2.2 (-8.1, 2.3)	0.08
MRI				
S_vO_2 [%]	55.2 (49.3, 60.2)	66.4 (57.0, 72.5)	13.2 (3.0, 18.2)	<0.001
OEF	0.38 (0.26,0.42)	0.19 (0.14, 0.24)	-51.6 (-59.9, -37.0)	<0.001
CBF (mL/minute per 100 g)	9.6 (7.5, 15.1)	21.9 (16.5, 31.0)	115.8 (83.5, 148.0)	<0.001
$CMRO_2$ (mL O_2/minute per 100 g)	0.49 (0.40, 0.79)	0.53 (0.40, 0.79)	4.6 (-31.8, 28.5)	0.68
Optics				
StO_2 (%)	49.3 (42.9, 54.7)	62.7 (51.5, 67.8)	11.1 (6.9, 19.1)	<0.001
OEF	0.58 (0.49, 0.68)	0.28 (0.19, 0.33)	-35.5 (-43.7, -26.7)	<0.001
BFI (10^{-9} cm^2/second)	17.8 (12.6, 27.0)	33.5 (23.9, 44.7)	75.0 (51.4, 87.0)	<0.001
CBV (mL/100 g)	1.74 (1.46, 2.08)	2.38 (2.05, 2.72)	37.3 (23.9, 45.7)	<0.001
$CMRO_{2i}$ (10^{-7} mL O_2/dL cm^2/second)	1.07 (0.88, 1.87)	1.23 (0.85, 1.99)	-7.3 (-21.0, 29.9)	0.86

BFI, blood flow index; C_a, arterial oxygen content; *CBF*, cerebral blood flow; *CBV*, cerebral blood volume; $CMRO_2$, cerebral metabolic rate of oxygen; $CMRO_{2i}$, $CMRO_2$ index; *Hb*, hemoglobin; *OEF*, oxygen extraction fraction; S_aO_2, arterial oxygen saturation; S_vO_2,venous oxygen saturation; StO_2, tissue oxygen saturation. Median and interquartile range of various hemodynamic parameters measured with MRI and optics at baseline and in response to hypercapnia. The *P* values were obtained from a Wilcoxon two-sided signed-rank test. *Determined from arterial blood gas analysis using co-oximetry.

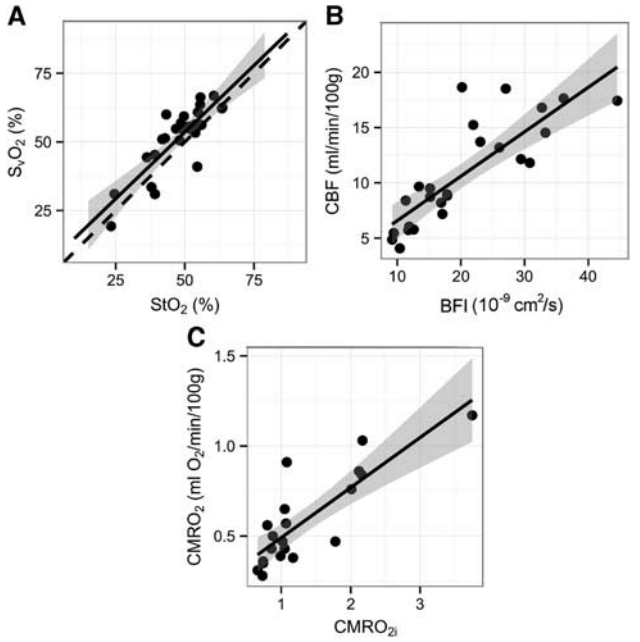

Figure 3. Correlations between resting-state magnetic resonance imaging and optical measurements: (**A**) venous oxygen saturation (S_vO_2) versus tissue oxygen saturation (StO_2); (**B**) cerebral blood flow (*CBF*) versus blood flow index (BFI); (**C**) cerebral oxygen consumption ($CMRO_2$) versus $CMRO_2$ index ($CMRO_{2i}$). The solid line represents the best linear fit to the data, while the dotted line indicates the line of identity. The gray ribbon denotes the 95% confidence interval for the linear fit. $CMRO_{2i}$ is in units of 10^{-7} mL O_2/dL cm^2/second.

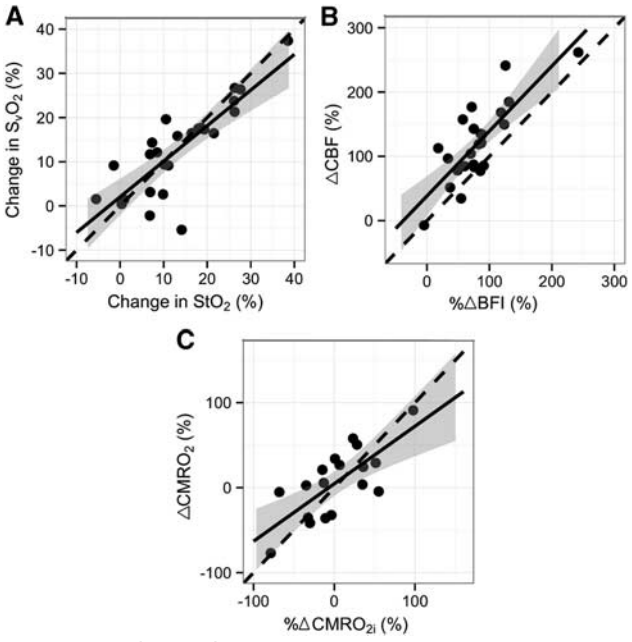

Figure 4. Correlations between magnetic resonance imaging and optical measurements in response to hypercapnia: (**A**) changes in oxygenation; (**B**) relative changes in cerebral blood flow (*CBF*) with respect to baseline; (**C**) relative changes in cerebral oxygen metabolism ($CMRO_2$) with respect to baseline. The solid line represents the best-fit line to the data, the dotted line indicates the line of identity. The gray ribbon denotes the 95% confidence interval for the linear fit.

Table 3. Linear relationships between MRI- and corresponding optics-based parameters

Parameter	*Slope (95% CI)*	*Intercept (95% CI)*	R^2, P-*value*
SvO_2	0.97 (0.71, 1.23)	5.1 (−7.6, 17.8)	0.69, $P<0.001$
CBF	0.40 (0.28, 0.52)	2.57 (−0.11, 5.25)	0.67, $P<0.001$
$CMRO_2$	0.28 (0.19, 0.37)	0.21 (0.07, 0.35)	0.67, $P<0.001$
ΔSvO_2	0.86 (0.64, 1.09)	1.0 (−2.8, 4.8)	0.71, $P<0.001$
ΔCBF	0.46 (0.21, 0.70)	5.1 (0.5, 9.7)	0.37, $P<0.001$
$\%\Delta CBF$	1.01 (0.68, 1.35)	38.3 (7.2, 69.4)	0.62, $P<0.001$
$\Delta CMRO_2$	0.31 (0.01, 0.62)	0.07 (−0.07, 0.2)	0.20, $P=0.055$
$\%\Delta CMRO_2$	0.57 (0.01, 1.13)	13.7 (−9.9, 37.5)	0.22, $P=0.046$

CBF, cerebral blood flow; CI, confidence interval; $CMRO_2$, cerebral metabolic rate of oxygen. Estimated slope and intercept for linear regression between MRI and optics-measured parameters along with the adjusted R^2 and *P* values. Here '%Δ' denotes relative change normalized to baseline values, while Δ denotes an absolute change.

difference between the two modalities' measures of relative changes and the slope was not significantly different from zero. Correlations between the absolute changes in *CBF* and $CMRO_2$ compared with absolute changes in BFI and $CMRO_{2i}$ were also computed (Table 3) and slopes of 0.46 (0.21, 0.70) and 0.31 (0.01, 0.62) were observed, respectively ($R=0.37$ and 0.39, $P=0.05$).

DISCUSSION

This work employs two novel noninvasive technologies, one based on MR and the other based on diffuse optics, to quantify cerebral oxygenation, perfusion, and $CMRO_2$ in a population of critically ill neonates with CHD undergoing cardiac surgery within the first month of life. The MR technique is sensitive to whole-brain macrovasculature, and the optical technique probes regional tissue microvasculature of the frontal cortex. Microvascular tissue oxygenation measures regional oxygen saturation whereas S_vO_2 quantifies the oxygen saturation of the blood in the major draining vein. The latter, along with S_aO_2 and a simultaneous measurement of *CBF*, provides the information needed to derive a global cerebral rate of oxygen consumption ($CMRO_2$).

In recent years, several noninvasive MR-based methods for quantification of absolute $CMRO_2$ quantification have been introduced to evaluate regional or global cerebral metabolism. The regional voxel-based methods model the effect of deoxygenated Hb in the capillary/post capillary bed on MR-measured transverse relaxation T_2 to quantify the voxel-wise oxygen saturation, which can be combined with ASL *CBF* measurement to yield $CMRO_2$. Among these are quantitative BOLD[9] and QUIXOTIC.[10] However, these methods involve complex models, are time intensive and numeric simulations and phantom experiments show that reliable estimates are achieved only in the presence of very high signal-to-noise ratio.

In contrast, methods that quantify oxygen extraction globally model the effect of deoxygenated Hb on the intravascular T_2 or MR signal phase of large veins to quantify intravascular S_vO_2, which combined with PC MR-based quantification of *CBF*, yield $CMRO_2$.[11,12,25] Although these methods provide global rather than spatially resolved measures, they are robust, and allow much higher temporal resolution and $CMRO_2$ quantification in clinically feasible scan times. Recently proposed methods such as phase-

based regional oxygen metabolism[14] and T_2 relaxation under spin tagging (TRUST)[9] fall under this category.

Our observations in anesthetized infants suggest that both MRI and optics-based techniques could be effectively integrated into future standard-of-care monitoring and management of critically ill neonates. Perhaps, most importantly, both techniques enable quantification of cerebral $CMRO_2$, a parameter that is critical to our understanding of oxygen utilization in the brain, especially in neonates with CHD who grow in an oxygen-starved environment and can suffer subsequent neurologic injury as a result. Measurements of $CMRO_2$ can help develop and guide treatment to ensure optimal oxygen utilization of the brain. Overall, baseline $CMRO_2$ in our cohort (Table 2) was 80% lower than typically observed in healthy adults, for whom values were reported in the range from 2 to 4 mL O_2/minute per 100 g.[13,26,27] Literature on $CMRO_2$ in neonates is scarce, due in part to the limited number of modalities available for use in very young children. In a study using PET in critically ill neonates from the neonatal intensive care unit, Altman *et al*[28] noted $CMRO_2$ values of 0.06 to 0.54 mL O_2/100 g per minute in preterm infants and 0.4 to 1.3 mL O_2/100 g per minute in sick term infants. Thus, our baseline $CMRO_2$ values (Table 2) are lower than those in the sick neonates, but close to those observed in the preterm neonates who tend to have a high incidence of hypoxic–ischemic brain injury in the form of periventricular leukomalacia and are therefore somewhat similar to our term neonates with CHD.

Furthermore, using these MRI- and optics-based techniques, we quantified *CBF*, *CBV*, and cerebral tissue and venous oxygenation. Unlike $CMRO_2$, which is very rarely quantified in infants, the former parameters are cited in literature more often; however, the techniques used to quantify these parameters are typically invasive, employing arterial or venous blood draws or the use of radioactive tracers. We observed a median resting-state *CBF* of 9.58 mL/minute per 100 g ~ 20% of normal adult *CBF*, which is typically around 50 mL/minute per 100 g,[13,26,27] and ~ 30% to 50% of healthy neonatal *CBF* in the frontal cortex, which Chiron *et al* reported as 34 ± 3.5 mL/minute per 100 g (using SPECT with ^{133}Xe) and Miranda *et al*. reported as 16.6 ± 5.9 mL/minute per 100 g (using arterial spin labeled perfusion MRI, ASL pMRI).[29,30] Licht *et al*[7] measured *CBF* with ASL perfusion MRI in a similar population of 25 term infants with CHD, found average resting *CBF* of 19.73 ± 9.15 mL/minute per 100 g, or approximately twice our current reported values. It bears mentioning that ASL pMRI has low intrinsic signal-to-noise ratio,[31,32] a problem that is exacerbated in very low-flow states, which is why ASL pMRI was not employed in this study.[31,33] The problem is further aggravated at 1.5T preventing accurate ASL measurements of *CBF*. Our current *CBF* values are more similar to those of preterm infants, which Pryds *et al*[34] reported as 10 ± 4 mL/minute per 100 g in a cohort of preterm neonates with a mean gestational age of 30.2 ± 2.8 weeks using intravenous ^{133}Xe clearance.[30,34] Similarly, we observed a median cerebral blood volume of 1.74 mL/100 g in our cohort, which is substantially lower than the cerebral blood volume measured by Ijichi *et al*.[22] using near-infrared spectroscopy in term neonates, although it is closer to the cerebral blood volumes they measured in preterm infants at 30 to 32 weeks postconceptual age.

Owing to a lack of longitudinal measurements in this CHD population, it is not possible to determine if the low *CBF* measures are secondary to low demand (low $CMRO_2$) or conversely, whether the low demand is a consequence of low oxygen delivery during brain development. Studies comparing CHD infants to other term infants without CHD include an MR spectroscopy study, which revealed striking structural and biochemical immaturity of the white matter in infants with CHD.[35] Licht *et al*[36] used a semi-quantitative observational scale to compare the maturation patterns seen in anatomic brain MRIs and demonstrated that the brain structures in infants with CHD were similar to preterm infants born at 35 weeks of gestation. In addition, Limperopoulos *et al*[37] used fetal MRI data to demonstrate a lag in brain growth during the third trimester of fetal development. We posit that the apparent delay in cerebral maturation is due to the alteration in fetal oxygen delivery to the brain that occurs as a consequence of the CHD anatomy. Taken together, our data suggest that *CBV*, *CBF*, and $CMRO_2$ in term infants with CHD are closer to the values obtained in preterm than healthy term infants.

Consistent with the known vasodilatory effects of CO_2, we observed an increase in *CBF* with hypercapnia ($P < 0.001$; Table 2), suggesting that CO_2 reactivity is intact in this cohort. Global $CMRO_2$ measured with both MRI and DOS/DCS showed no population-averaged change due to hypercapnia. This observation agrees with our previous experience in healthy adults[20] and with several other publications that examined cerebrovascular reactivity to hypercapnia in patients with congenital heart defects using localized measurement techniques, such as DOS and DCS.[15,24,38]

In addition to generating new physiologic data, this work also achieved several technical goals. First, it demonstrates the feasibility of a combined MRI-susceptometry and phase-contrast method to measure S_vO_2, *CBF* and $CMRO_2$, in neonates with complex CHD, all in absolute physiologic units. Second, the absolute normocapnic MRI measurements were tightly correlated with optical DOS/DCS indices of regional blood flow and $CMRO_2$. Transport to MRI is not always feasible, e.g., a neonate with hemodynamic instability or dependent on technologies such as an external pacemaker or extracorporeal membrane oxygenation. Therefore, the strong correlations of MRI and optical methods provide useful new calibration factors for optical techniques in this patient group, and they suggest that DOS/DCS may prove valuable as a portable bedside monitor to assess cerebral perfusion and oxygen utilization. We note that the calibration factors derived are strictly valid only for the specific population studied and thus studies in related (e.g., healthy age-matched) populations will be needed. The present work illustrates how such measurements should be carried out and provides a useful point of comparison for future measurements in related populations. Furthermore, many similarities exist between the normal and diseased populations that might not change with disease from the standpoint of the optical measurements, e.g., head geometry, average tissue absorption, and scattering, etc. For this reason, the calibrations presented may offer a useful 'first' approximation for related populations.

Interestingly, the correlations observed between MRI and optical methods were strong even though the techniques have different spatial and physiologic sensitivities. For example, MRI-susceptometry measures venous oxygenation (S_vO_2) whereas DOS measures regional tissue microvasculature oxygenation (StO_2), which is a weighted average of arterial, capillary, and venous oxygenation levels. Additionally, the optical BFI depends on the motion and concentration of red blood cells and is thus a surrogate measure of regional *CBF* in the microvasculature of the frontal cortex; by contrast, the MRI-measured *CBF* derives its macrovascular signal from the draining veins of the whole brain, with bias to the cortical mantle.

Notwithstanding these differences, the correlations between baseline S_vO_2 and StO_2, and baseline *CBF* and BFI were robust (Figure 3). Perhaps, somewhat surprisingly, the values of S_vO_2 were higher or equal to the StO_2. One might expect S_vO_2 to be lower than StO_2, as the latter has an arterial contribution. However, some discordance between the two measurements might also be expected, because the optical probe measures focal hemodynamics over the frontal areas of the brain, which tend to be hypometabolic in neonates.[39] Finally, the measured values of StO_2 agree very well with those previously reported by Kurth *et al*[40] in nonanesthetized CHD infants.

Furthermore, although correlation between relative changes in *CBF* and BFI due to hypercapnia was highly significant ($R^2 = 0.67$,

$P < 0.001$), the optically measured %ΔBFI tended to underestimate the MRI-measured %Δ*CBF*. This underestimation is potentially due to the regional heterogeneity in cortical cerebrovascular response to hypercapnia.[41] In adults, cerebrovascular reactivity among frontal, parietal, temporal, and occipital cortices has been measured to vary substantially;[41] thus, changes in frontal cortex *CBF* measured with DCS need not correlate in a 1:1 fashion with changes in global venous flow in the SSS measured with MRI. Alternatively and/or additionally, the underestimation of %ΔBFI compared with %Δ*CBF* may be due to the effects of extracerebral layers on the DCS signal. One might expect, however, that at large, source-detector separations and for hypercapnic functional perturbations, the changes measured by diffuse optics should be mostly occurring in the deeper tissues and should therefore be least susceptible (i.e. compared with baseline measurements) to be different from changes observed by MRI.

Limitations

One obvious limitation of our study is the lack of healthy control subjects. Nevertheless, both MRI and optical techniques can readily be employed in healthy neonates, and recruitment of age-matched healthy neonates will be the subject of future studies. Furthermore, anesthetic effects could mask true resting-state values of cerebral hemodynamics in our CHD cohort. However, sedation and paralysis were achieved with fentanyl and pancuronium, both of which have been demonstrated to have minimal effects of *CBF* and $CMRO_2$ in animal models.[42–44]

Although our initial experience with MRI- and optics-based $CMRO_2$ quantification in neonates with complex CHD has been encouraging, each technique presents its own limitations. We discuss limitations with the MRI technique first. The accuracy of MRI-measured S_vO_2 quantification depends on $\Delta\chi_{do}$, which has been previously determined using healthy adult blood.[17,45] It is plausible that this constant might differ slightly for fetal blood given the presence of fetal Hb. However, it is unlikely that the inherent paramagnetism of heme iron in its deoxy state in fetal Hb is substantially different from that in adult Hb as the two Hb types differ only in the type of globin chains present. Good agreement with optical data (Figures 3 and 4) gives us confidence that these sorts of corrections, i.e. due to potential differences in magnetic properties of fetal Hb, are small. In a different vein, the S_vO_2, *CBF*, and $CMRO_2$ measurements presented herein still require arterial blood samples. However, even though pulse oximetry offers a noninvasive measure of peripheral oxygen saturation as a possible alternative to blood gas analysis, for this cohort of cyanotic neonates, pulse oximetry measures are also subject to errors. Blood flow in the SSS, which drains only the cortical mantle, was used to determine total *CBF*, based on recent work showing that the SSS accounts for 45% of total *CBF* as pointed out earlier.[19]

Finally, the MRI measurements require transport and are not amenable to bedside monitoring; however, once in-magnet, the pulse sequences employed permit rapid quantification of cerebral hemodynamics (<5 minutes including localizer scans) and can be conveniently added to standard clinical protocols without additional time penalties.

The diffuse optical spectroscopies have limitations as well. Generally, the optical methods are limited to probing shallow depths in the frontal cortex in the region under the optical probe. In this study, we presumed and corroborated that diffuse optical frontal cortex measurements produce physiologic parameters that are indicative of whole-brain resting state and hypercapnic responses (e.g., as measured by MRI). In general, this assumption may not be true, e.g., in disease states such as stroke or hemorrhage; in addition, the study of regional responses is interesting in its own right. Further, as mentioned above, in studies of human brain, optical techniques are also sensitive to the responses of extracerebral tissues such as scalp and skull. To alleviate the potential issues of extracerebral signal contamination, two- and multilayer analysis models can be employed, and physical perturbations such as increased probe pressure can be used to maximize cerebral signals; this problem is an issue of current research interest. Finally, the blood flow indices are not absolute. Again, however, studies such as the present one offer a means to calibrate DCS indices in particular patient populations and, of course, functional activation and/or perturbation responses do not require absolute indices.

CONCLUSION

In summary, using MRI and optical techniques, we noninvasively quantified suppressed cerebral oxygenation, flow, and $CMRO_2$ in neonates with complex CHD as compared with literature values for controls. The findings of strikingly low *CBF* and $CMRO_2$ are in keeping with the observations made by this group and others, i.e. the brains of term infants with severe forms of CHD are immature and more similar to the brains of premature infants. Furthermore, we confirmed CO_2 reactivity in these patients is intact, and we observed significant correlations between MRI-measured S_vO_2, *CBF*, and $CMRO_2$ with optical measurements (StO_2, BFI, $CMRO_{2i}$) both at rest and during hypercapnia. These results suggest MRI and optical measurements of cerebral hemodynamics parallel one another for evaluation and management of critically ill CHD neonates.

DISCLOSURE/CONFLICT OF INTEREST

The authors declare no conflict of interest.

REFERENCES

1 Volpe JJ. Neurobiology of periventricular leukomalacia in the premature infant. *Pediatr Res* 2001; **50**: 553–562.
2 Back SA, Han BH, Luo NL, Chricton CA, Xanthoudakis S, Tam J *et al.* Selective vulnerability of late oligodendrocyte progenitors to hypoxia-ischemia. *J Neurosci* 2002; **22**: 455–463.
3 Bellinger DC, Wypij D, duPlessis AJ, Rappaport LA, Jonas RA, Wernovsky G *et al.* Neurodevelopmental status at eight years in children with dextro-transposition of the great arteries: the Boston Circulatory Arrest Trial. *J Thorac Cardiovasc Surg* 2003; **126**: 1385–1396.
4 Wernovsky G, Shillingford AJ, Gaynor JW. Central nervous system outcomes in children with complex congenital heart disease. *Curr Opin Cardiol* 2005; **20**: 94–99.
5 Buckley EM, Cook NM, Durduran T, Kim MN, Zhou C, Choe R *et al.* Cerebral hemodynamics in preterm infants during positional intervention measured with diffuse correlation spectroscopy and transcranial Doppler ultrasound. *Opt Express* 2009; **17**: 12571–12581.
6 Romagnoli C, Giannantonio C, De Carolis MP, Gallini F, Zecca E, Papacci P. Neonatal color Doppler US study: normal values of cerebral blood flow velocities in preterm infants in the first month of life. *Ultrasound Med Biol* 2006; **32**: 321–331.
7 Licht DJ, Wang J, Silvestre DW, Nicolson SC, Montenegro LM, Wernovsky G *et al.* Preoperative cerebral blood flow is diminished in neonates with severe congenital heart defects. *J Thorac Cardiovasc Surg* 2004; **128**: 841–849.
8 Pelc NJ, Bernstein MA, Shimakawa A, Glover GH. Encoding strategies for three-direction phase-contrast MR imaging of flow. *J Magn Reson Imag* 1991; **1**: 405–413.
9 Lu H, Ge Y. Quantitative evaluation of oxygenation in venous vessels using T2-Relaxation-Under-Spin-Tagging MRI. *Magn Reson Med* 2008; **60**: 357–363.
10 Bolar DS, Rosen BR, Sorensen AG, Adalsteinsson E. QUantitative Imaging of eXtraction of oxygen and TIssue consumption (QUIXOTIC) using venular-targeted velocity-selective spin labeling. *Magn Reson Med* 2011; **66**: 1550–1562.
11 Haacke EM, Lai S, Reichenbach JR, Kuppusamy K, Hoogenraad FGC, Takeichi H *et al. In vivo* measurement of blood oxygen saturation using magnetic resonance imaging: a direct validation of the blood oxygen level-dependent concept in functional brain imaging. *Hum Brain Mapp* 1997; **5**: 341–346.
12 Fernández-Seara M, Detre JA, Techawiboonwong A, Wehrli FW. MR susceptometry for measuring global brain oxygen extraction. *Magn Reson Med* 2006; **55**: 967–973.

13 Jain V, Langham MC, Wehrli FW. MRI estimation of global brain oxygen consumption rate. *J Cereb Blood Flow Metab* 2010; **30**: 1598–1607.
14 Fan AP, Benner T, Bolar DS, Rosen BR, Adalsteinsson E. Phase-based regional oxygen metabolism (PROM) using MRI. *Magn Reson Med* 2012; **67**: 669–678.
15 Durduran T, Zhou C, Buckley EM, Kim MN, Yu G, Choe R *et al.* Optical measurement of cerebral hemodynamics and oxygen metabolism in neonates with congenital heart defects. *J Biomed Opt* 2010; **15**: 037004.
16 Buckley EM, Lynch JM, Goff DA, Schwab PJ, Baker WB, Durduran T *et al.* Early postoperative changes in cerebral oxygen metabolism following neonatal cardiac surgery: Effects of surgical duration. *J Thorac Cardiovasc Surg* 2013; **145**: e1.
17 Spees WM, Yablonskiy DA, Oswood MC, Ackerman JJ. Water proton MR properties of human blood at 1.5 Tesla: magnetic susceptibility, T(1), T(2), T*(2), and non-Lorentzian signal behavior. *Magn Reson Med* 2001; **45**: 533–542.
18 Stoquart-Elsankari S, Lehmann P, Villette A, Czosnyka M, Meyer ME, Deramond H *et al.* A phase-contrast MRI study of physiologic cerebral venous flow. *J Cereb Blood Flow Metab* 2009; **29**: 1208–1215.
19 Rodgers ZB, Jain V, Englund EK, Langham MC, Wehrli FW. High temporal resolution MRI quantification of global cerebral metabolic rate of oxygen consumption in response to apneic challenge. *J Cereb Blood Flow Metab* 2013; **33**: 1514–1522.
20 Jain V, Langham MC, Floyd TF, Jain G, Magland JF, Wehrli FW. Rapid magnetic resonance measurement of global cerebral metabolic rate of oxygen consumption in humans during rest and hypercapnia. *J Cereb Blood Flow Metab* 2011; **31**: 1504–1512.
21 Durduran T, Choe R, Baker WB, Yodh AG. Diffuse optics for tissue monitoring and tomography. *Rep Progr Phys* 2010; **73**: 1–43.
22 Ijichi S, Kusaka T, Isobe K, Okubo K, Kawada K, Namba M *et al.* Developmental changes of optical properties in neonates determined by near-infrared time-resolved spectroscopy. *Pediatr Res* 2005; **58**: 568–573.
23 Boas DA, Yodh AG. Spatially varying dynamical properties of turbid media probed with diffusing temporal light correlation. *J Optic Soc Am A* 1997; **14**: 192–215.
24 Buckley EM, Hance D, Pawlowski T, Lynch JM, Wilson FB, Mesquita RC *et al.* Validation of diffuse correlation spectroscopic measurements of cerebral blood flow using phase-encoded velocity mapping MRI. *J Biomed Opt* 2012; **17**: 037007.
25 Wright GA, Hu BS, Macovski A 1991I.I. Rabi Award. Estimating oxygen saturation of blood *in vivo* with MR imaging at 1.5 T. *J Magn Reson Imag* 1991; **1**: 275–283.
26 Leenders KL, Perani D, Lammertsma AA, Heather JD, Buckingham P, Healy MJ *et al.* Cerebral blood flow, blood volume and oxygen utilization. Normal values and effect of age. *Brain* 1990; **113**: 27–47.
27 Kety SS. Human cerebral blood flow and oxygen consumption as related to aging. *Res Publ Assoc Res Nerv Ment Dis* 1956; **3**: 31–45.
28 Altman DI, Perlman JM, Volpe JJ, Powers WJ. Cerebral oxygen metabolism in newborns. *Pediatrics* 1993; **92**: 99–104.
29 Chiron C, Raynaud C, Maziere B, Zilbovicius M, Laflamme L, Masure MC *et al.* Changes in regional cerebral blood flow during brain maturation in children and adolescents. *J Nucl Med* 1992; **33**: 696–703.
30 Miranda MJ, Olofsson K, Sidaros K. Noninvasive measurements of regional cerebral perfusion in preterm and term neonates by magnetic resonance arterial spin labeling. *Pediatr Res* 2006; **60**: 359–363.
31 Wu St WC, Lawrence KS, Licht DJ, Wang DJ. Quantification issues in arterial spin labeling perfusion magnetic resonance imaging. *Top Magn Reson Imag* 2010; **21**: 65–73.
32 Deibler AR, Pollock JM, Kraft RA, Tan H, Burdette JH, Maldjian JA. Arterial spin-labeling in routine clinical practice, part 1: technique and artifacts. *AJNR Am J Neuroradiol* 2008; **29**: 1228–1234.
33 Goff DA, Buckley EM, Durduran T, Wang J, Licht DJ. Noninvasive cerebral perfusion imaging in high-risk neonates. *Semin Perinatol* 2010; **34**: 46–56.
34 Pryds O, Greisen G, Skov LL, Friis-Hansen B. Carbon dioxide-related changes in cerebral blood volume and cerebral blood flow in mechanically ventilated preterm neonates: comparison of near infrared spectrophotometry and ^{133}Xenon clearance. *Pediatr Res* 1990; **27**: 445–449.
35 Miller SP, McQuillen PS, Hamrick S, Xu D, Glidden DV, Charlton N *et al.* Abnormal brain development in newborns with congenital heart disease. *N Engl J Med* 2007; **357**: 1928–1938.
36 Licht DJ, Shera DM, Clancy RR, Wernovsky G, Montenegro LM, Nicolson SC *et al.* Brain maturation is delayed in infants with complex congenital heart defects. *J Thorac Cardiovasc Surg* 2009; **137**: 529–536, discussion 536-537.
37 Limperopoulos C, Tworetzky W, McElhinney DB, Newburger JW, Brown DW, Robertson Jr. RL *et al.* Brain volume and metabolism in fetuses with congenital heart disease: evaluation with quantitative magnetic resonance imaging and spectroscopy. *Circulation* 2010; **121**: 26–33.
38 Ramamoorthy C, Tabbutt S, Kurth CD, Steven JM, Montenegro LM, Durning S *et al.* Effects of inspired hypoxic and hypercapnic gas mixtures on cerebral oxygen saturation in neonates with univentricular heart defects. *Anesthesiology* 2002; **96**: 283–288.
39 Lin PY, Roche-Labarbe N, Dehaes M, Fenoglio A, Grant PE, Franceschini MA. Regional and hemispheric asymmetries of cerebral hemodynamic and oxygen metabolism in newborns. *Cereb Cortex* 2012; **23**: 339–348.
40 Kurth CD, Steven JL, Montenegro LM, Watzman HM, Gaynor JW, Spray TL *et al.* Cerebral oxygen saturation before congenital heart surgery. *Ann Thorac Surg* 2001; **72**: 187–192.
41 Ito H, Yokoyama I, Iida H, Kinoshita T, Hatazawa J, Shimosegawa E *et al.* Regional differences in cerebral vascular response to PaCO2 changes in humans measured by positron emission tomography. *J Cereb Blood Flow Metab* 2000; **20**: 1264–1270.
42 Milde LN, Milde JH, Gallagher WJ. Cerebral effects of fentanyl in dogs. *Br J Anaesth* 1989; **63**: 710–715.
43 Belik J, Wagerle LC, Delivoria-Papadopoulos M. Cerebral blood flow and metabolism following pancuronium bromide in newborn lambs. *Pediatr Res* 1984; **18**: 1305–1308.
44 Carlsson C, Hagerdal M, Kaasik AE, Siesjo BK. A catecholamine-mediated increase in cerebral oxygen uptake during immobilisation stress in rats. *Brain Res* 1977; **119**: 223–231.
45 Jain V, Abdulmalik O, Propert KJ, Wehrli FW. Investigating the magnetic susceptibility properties of fresh human blood for noninvasive oxygen saturation quantification. *Magn Reson Med* 2012; **68**: 863–867.
46 Watzman HM, Kurth CD, Montenegro LM, Rome J, Steven JM, Nicolson SC. Arterial and venous contributions to near-infrared cerebral oximetry. *Anesthesiology* 2000; **93**: 947–953.
47 Culver JP, Durduran T, Furuya D, Cheung C, Greenberg JH, Yodh AG. Diffuse optical tomography of cerebral blood flow, oxygenation, and metabolism in rat during focal ischemia. *J Cereb Blood Flow Metab* 2003; **23**: 911–924.

Supplementary Information accompanies the paper on the Journal of Cerebral Blood Flow & Metabolism website (http://www.nature.com/jcbfm)

APPENDIX 1

A complication of the DOS/DCS measurement and analysis protocol was that the optical probe employed to quantify absolute DOS baseline parameters was not MRI compatible. First, a baseline DOS measurement, made just before the patient's entrance into the MRI scanner, was carried out with a custom-made rubber probe with four DOS source-detector separations of 1.5, 2.0, 2.5, 3.0 cm, and two NIR laser source wavelengths, 686 and 830 nm (ISS, Urbana Champaign, IL, USA). The four source-detector pairs probe different depths in the tissue and are needed/used to improve the absolute accuracy of tissue property assignments. These measurements had to be done outside of the MRI because the optical probe contained prisms with metallic coatings that are not MRI compatible.

These DOS baseline measurements employed diffusion theory in the semi-infinite geometry with extrapolated boundary conditions for analysis.[21] Measurements were made over the frontal cortex. Cerebral blood volume (*CBV*) and *OEF* were quantified using SaO_2 and *Hb* from baseline arterial blood samples obtained once the patient was in the MRI:

$$CBV \quad \frac{MW_{\mathrm{Hb}} \quad THC}{D_{\mathrm{bt}} \quad Hb} \qquad (1)\leftarrow$$

Here $MW_{\mathrm{Hb}} = 64{,}500$ g/mol is the molecular weight of Hb, D_{bt} is the brain tissue density (assumed 1.05 g/mL), and *Hb* is the arterial Hb concentration (g/dL) measured in arterial blood samples. Furthermore, we define *OEF* as[21]

$$OEF \quad \frac{1}{\gamma}\frac{SaO_2 - StO_2}{SaO_2} \qquad (2)\leftarrow$$

SaO_2 (%) is the arterial oxygen saturation, and $\gamma = 0.75$ represents the fraction of blood volume contained in the venous

compartment of the probed tissue (assumed constant).[46,47] This baseline measurement protocol and corresponding data analysis are more fully described in reference.[16]

Next, the patient was placed in the MRI scanner; here, continuous DCS measures of tissue BFI as well as DOS measured changes in chromophore concentrations were acquired by a different MRI-compatible optical probe that employed a 2.5 cm source-detector configuration for both DOS and DCS. In practice, photons from this source-detector configuration interrogate a region $\sim$1 to 1.5 cm below the scalp, i.e., the surface region of the frontal cortex. The DOS sub-component in the MRI scanner continuously measured relative changes in tissue physiologic properties before and during hypercapnia, and the corresponding DCS sub-component yielded absolute BFI throughout the MRI scan.

The DOS component of the in-magnet monitoring employed the modified Beer–Lambert law[21] for semi-infinite media to derive hypercapnia-induced changes (Δ) in HbR, HbO_2, and THC as a function of time from corresponding changes in detected light intensity at 686 nm, 786 nm, and 830 nm. Mean changes due to hypercapnia for each patient, i.e., ΔHbR, ΔHbO_2, and ΔTHC, were calculated by averaging these parameters during the $\sim$1-minute room-air and hypercapnia MRI scans. Average absolute hypercapnic *CBV* and StO_2 values were then derived using the preMRI absolute measurements, along with the average changes (Δ) due to hypercapnia in HbO_2 and THC measured in-magnet, i.e.,

$$CBV_{CO_2} = \frac{MW_{Hb}}{D_{bt}} \frac{(THC + \Delta THC)}{Hgb_{CO_2}} \quad (3)$$

$$StO_{2_{CO_2}} = \frac{HbO_2 + \Delta HbO_2}{THC + \Delta THC} \quad (4)$$

Here Hgb_{CO_2} is the arterial Hb value quantified during the hypercapnia blood draw. Hypercapnic *OEF* was quantified using hypercapnic SaO_2 and StO_2 via equation (2).

The DCS component of the in-magnet monitoring employed fits to the analytical solution of the correlation diffusion equation with the standard semi-infinite boundary conditions to derive continuous DCS data (i.e., BFI) throughout the hypercapnia protocol.[21] The DOS data provided absolute tissue absorption coefficient needed for optimal fitting of DCS autocorrelation curves (see Supplementary Materials for more information on the effects of the tissue reduced scattering coefficient on BFI).